Draft project on CAP modeling

François Deloche

March 19, 2020

1 Elements from previous work

Note: Good review article on CAP
Ups and downs in 75 years of electrocochleography Eggermont [Eggermont, 2017].

1.1 The narrow-band contributions to the compound action potential

Masking of a click or tone-burst with a high-passed white noise (NB: not strictly speaking forward masking as the noise was kept during the probe, as far as I understand). The subtraction of the CAP obtained with masking with the previous recording (f_{cut} cut-off frequency decreases at each step) gives the 'narrow-band' contribution of the CAP.

It has been used especially by Eggermont, although not the 1st one to use it (Teas et al., 1962)

- *Analysis of compound action potential responses to tone bursts in the human and guinea pig cochlea* Eggermont 1976 [Eggermont, 1976]
  - TT recordings
- *Narrow-band analysis of compound action potentials for several stimulus conditions in the guinea pig* Eggermont 1981

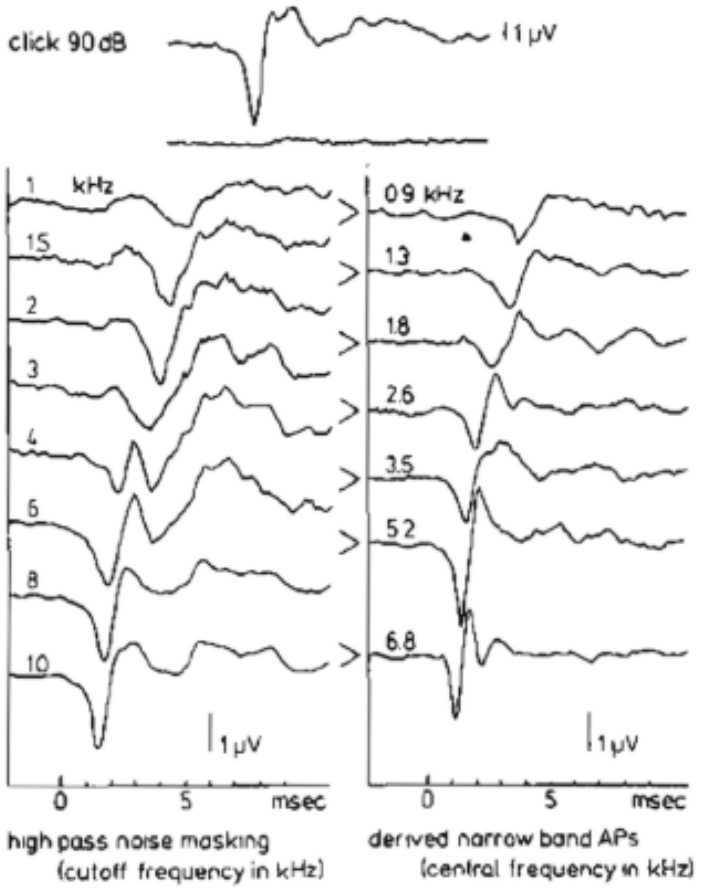

FIGURE 9 | High-pass noise masking and the derivation of narrow band APs (NAPs) in humans. The upper two traces show the whole nerve CAP for a normal ear in response to a 90 dB p.e. SPL click and reflect the situation where just complete masking by wide-band noise occurs. On the left hand side the effect of high-passing the noise at successively higher cut-off frequencies can be seen. Subtraction of two subsequent CAP's results in the set of narrow-band CAP's in the right-hand side. From Eggermont (1979c).

Figure 1: NAP of click in humans

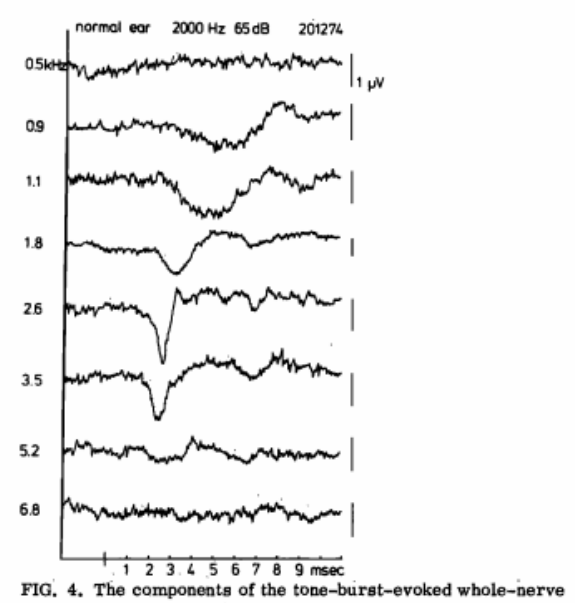

FIG. 4. The components of the tone-burst-evoked whole-nerve AP. In contrast to the click data, here the maximum contribution to the AP originates from the 2.6-kHz region, and contributions from the 5.2-kHz region (which dominate the click AP) and higher may be neglected. The diphasic shape is less obvious than for the click responses.

Figure 2: NAP of tone burst in humans. Eggermont 1976

Note: He found quite a different pattern for NAP in response to tone bursts in guinea pigs (second negative peak)

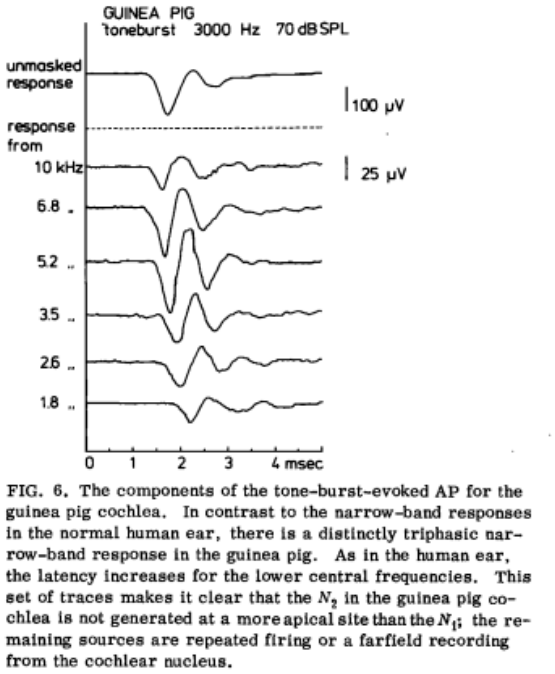

FIG. 6. The components of the tone-burst-evoked AP for the guinea pig cochlea. In contrast to the narrow-band responses in the normal human ear, there is a distinctly triphasic narrow-band response in the guinea pig. As in the human ear, the latency increases for the lower central frequencies. This set of traces makes it clear that the N_2 in the guinea pig cochlea is not generated at a more apical site than the N_1; the remaining sources are repeated firing or a farfield recording from the cochlear nucleus.

Figure 3: NAP of tone burst in guinea pigs. Eggermont 1976

Seems like we see a broader tuning of auditory filters.

- more frequencies contribute to the CAP
- also the 'narrow-band analysis' is less frequency selective. In fact, the 'NAPs' do not show exactly the contribution of each frequency band because of the spread of the masker along the cochlear partition (this problem is alleviated in the model I propose because it seeks to estimate this spread with tuning of auditory filters)

The NAP method was used to estimate the latencies of each frequency contribution:

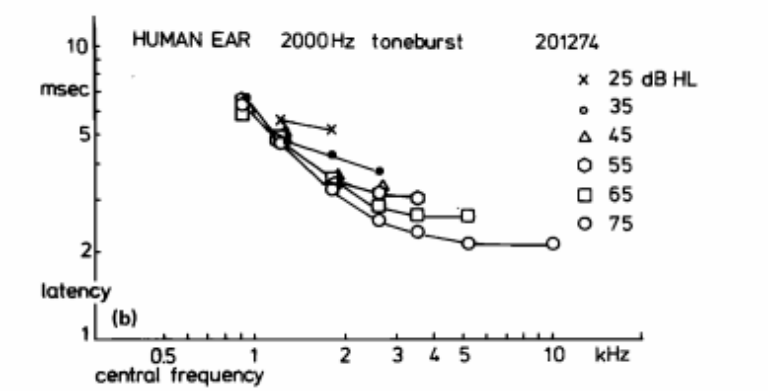

Figure 4: Latencies estimated with the NAP method

(exponential dependency on distance steps, more visible on this figure for click :)

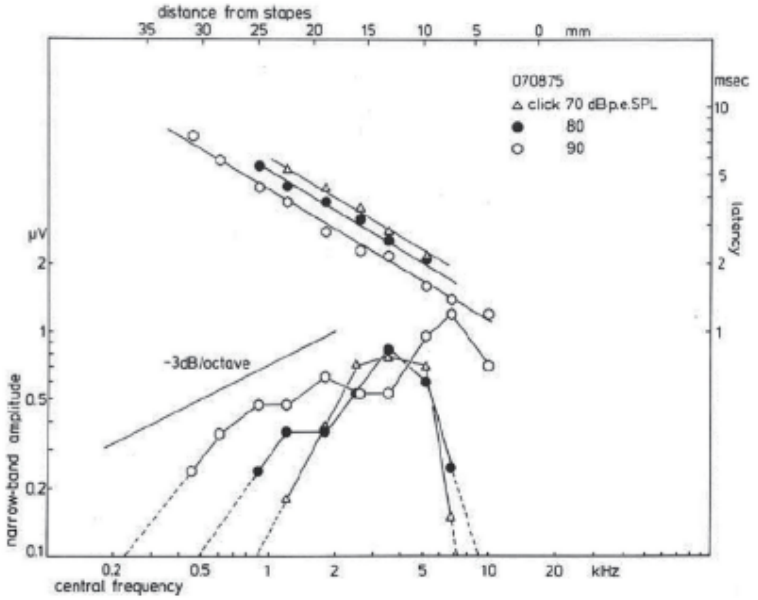

FIGURE 10 | Narrow band response parameters as a function of central frequency (CF). For clicks of 70, 80, and 90 dB p.e. SPL, narrow band amplitudes are shown as a function of distance from the stapes; it is observed that for the highest intensity the amplitudes decrease by about 3 dB/octave. Lowering the click intensity results in a decrease for contributions from both the apical and basal part of the cochlea, while the central part still contributes the same. The latency data show an exponential dependency on the distance from the stapes, and a definite effect of stimulus intensity thereupon is noted. From Eggermont (1976c).

Figure 5: Latencies estimated with the NAP method

1.2 Unit responses, convolution models

- Individual ANF contribution

From Eggermont 2017 (review article):

> Further experimental evidence for the applicability of the NAP technique in pathological cochleas came from recordings in normal and noise-exposed guinea pigs (Versnel et al., 1992), which looked at the validity of using the same unit response along the CF range and in normal vs. hearing loss ears. They used a technique pioneered by Kiang et al. (1976) involving spike-triggered averaging of round window "noise". In that way one can estimate the unit response for units with CFs corresponding to locations along the cochlear partition. Their findings in normal cochleas confirmed the earlier data from Prijs (1986), namely that the unit response was diphasic and had a fairly constant amplitude of about 0.1 µV. In noise-exposed cochleas, waveform, latency and amplitude of the negative component of the unit response remained unchanged.

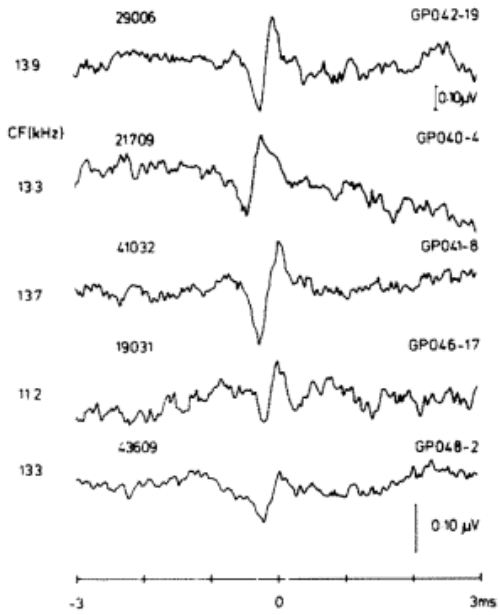

Fig. 4. Five examples of aps for fibres with almost identical CF in different animals. Computations were based on spontaneous activity. The number of counts is indicated on the left, above each trace. In GP 040 and GP 041 triggering occurred at the leading edge, in the other GPs at the back edge.

Figure 6: Unit response estimated with spike-triggered average, Prijs 1986 [Prijs, 1986]

Similar to Kiang et al. 1976 [Kiang et al., 1976].

Other ref: thesis of Wang [Wang, 1979]

Note: interpretation in terms of finite differences: $\approx \delta - 2/1000\delta'$ (and possibly second derivative)

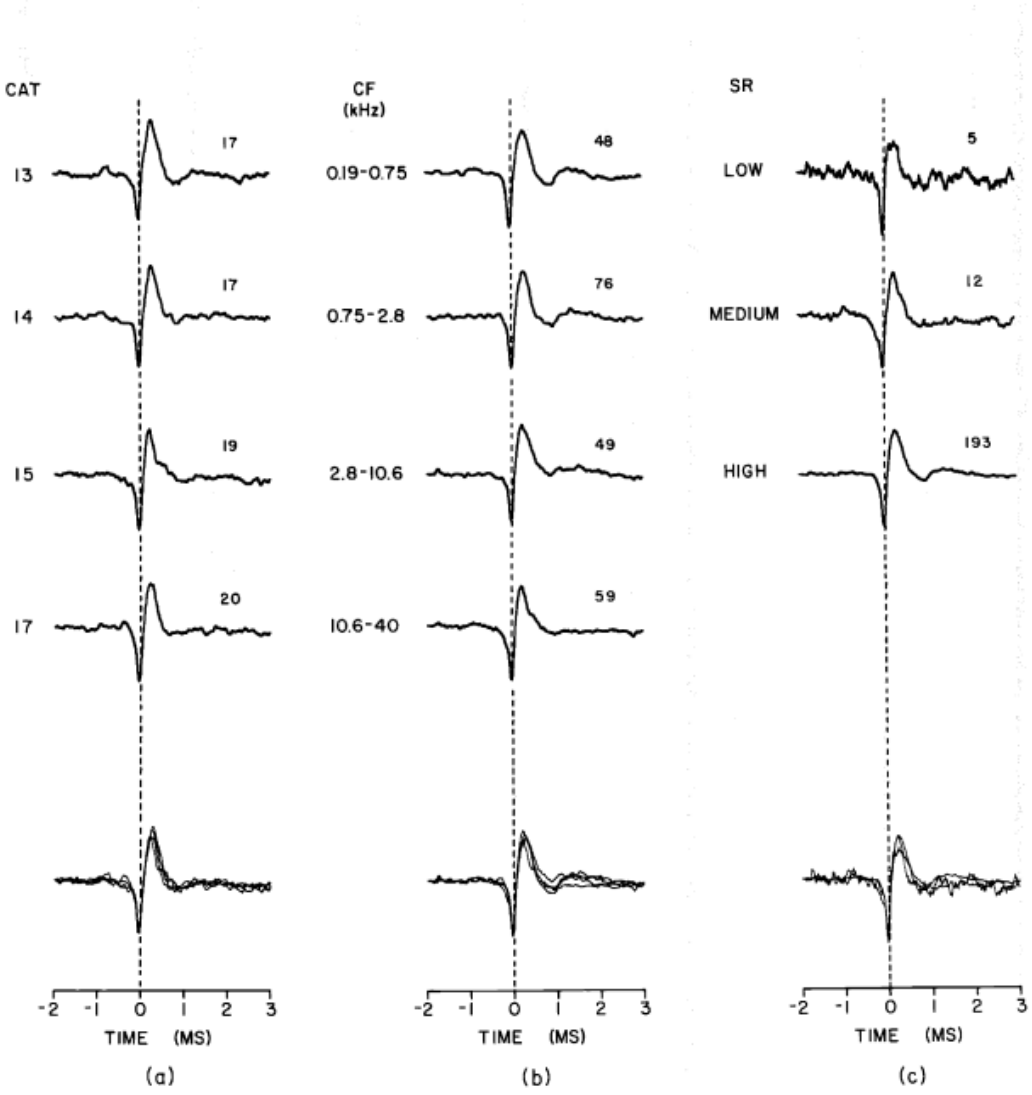

Figure 7: Fig 13 [Wang, 1979] : averages of URs depending on animal, CF, SR

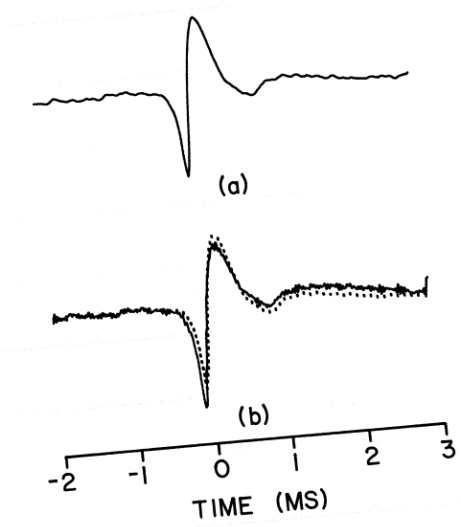

Figure 8: Fig 14 [Wang, 1979] : full average

- Synchronous fibers contribution

Related to the PST histogram or time distribution of first spike (if 2nd peak negligible)

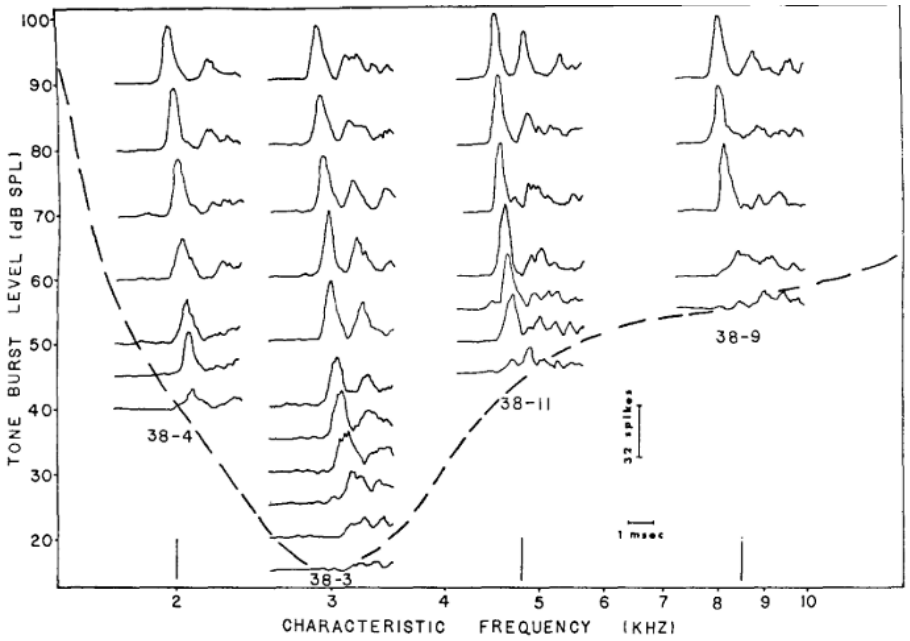

Fig. 4. Onset PST histograms of 4 fibers in response to tone bursts of 3 kHz. The histograms are positioned according to logarithmic frequency and intensity scales. The dashed line shows the approximate 3 kHz across-fiber tuning curve.

Figure 9: Contributions of several ANFs at the onset of a tone. [Özdamar and Dallos, 1978]

- Double convolution models (or similar)
  - *Synthetic whole-nerve action potentials for the cat* E. de Boer 1975 artifical PST histograms are computed with a filter + envelope + rectifier model, so it seems to go far in the modeling
  - *Deconvolution of compound action potentials and nonlinear features of the PST histogram* [Bappert et al., 1980]

$$CAP = \underbrace{E \star NPST}_{CPST} \star UR$$

CAP:Compound action potential
E: excitation pattern (in time, does not try to go in the frequency domain using the latencies)
NPST: "norm" PST (distribution of spikes for synchronous ANFs)
CPST: Compound PST (PST given all the contributions of ANFs)
UR: unit response
In fact, there is a logarithm transform (dilatation) of the CPST to take into account the exponential shape of latencies wrt distance stapes, so it is not strictly speaking a double convolution.
The model was used to estimate the excitation pattern.

1.3 Forward masking experiments

- *AP responses in forward-masking paradigms and relationship to responses of auditory-nerve fibers* Abbas, JASA 1981 [Abbas and Gorga, 1981]
- Verschooten et al., 2012/2018 [Verschooten et al., 2012, 2018]
- *Forward masking of the compound action potential: Thresholds for the detection of the N1 peak* Relkin 1990 (deals with detection threshold and % detection only) [Relkin and Smith, 1991]
- estimation of tuning : Harrison 1981 [Harrison et al., 1981b,a], Verschooten et al.

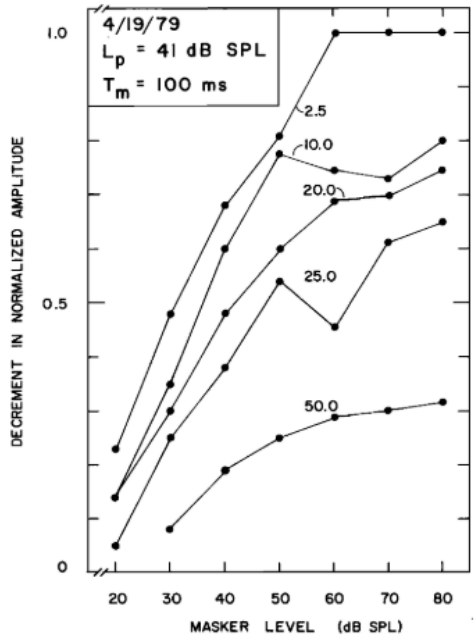

FIG. 3. Decrement in normalized amplitude is plotted as a function of level of masking tone. Parameter is Δt expressed in ms. Data are the same as those in Fig. 2.

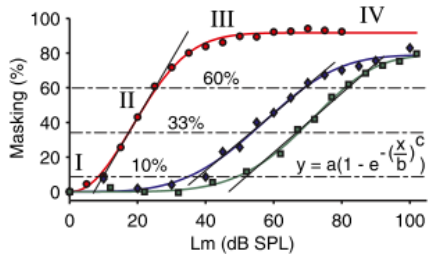

FIG. 5. Masking intensity curves, amount of masking as a function of masker level, for different conditions in two different cats. The masking curves are fits of cumulative Weibull distribution functions (formula included in the figure). The conditions for the curves are, from *left* to *right*: *red-filled dots*, L_p=40 dB SPL, f_p=10 kHz, nNW=0, a=91.68, b=24.89, c=2.129, animal 1; *blue diamonds*, L_p=67 dB SPL, f_p=2 kHz, nNW=0.44, a=78.89, b=62.62, c=3.668, animal 2; and *green squares*, L_p=60 dB SPL, f_p=6 kHz, nNW=0.34, a=78.72, b=75.29, c=5.031, animal 2. Four different regions can be identified: I, region with almost no masking; II, region with a steep linear growth (on semi-log plot, *solid lines*), i.e., between ~10 and 60 % masking (*upper and lower horizontal dashed dotted lines*); III, transition region with a much smaller growth; and IV a region clipped to maximal masking. The middle of region II is the best region for the masking criterion, chosen at ~33 % (*middle horizontal dashed dotted line*).

Abbas et al.

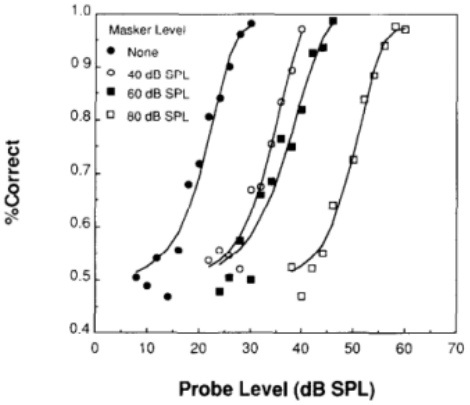

Fig. 2. Neurometric functions for the detection of the probe. Masker level is indicated by the symbols as shown on the figure. Solid lines are best-fit Weibull functions. The maskers produce a nearly parallel shift of the functions to the right along the abscissa. Masked threshold shift is defined as the distance between the Weibull function for the masked and unmasked conditions at 75% correct detection probability.

Relkin 1990

Verschooten et al. 2012

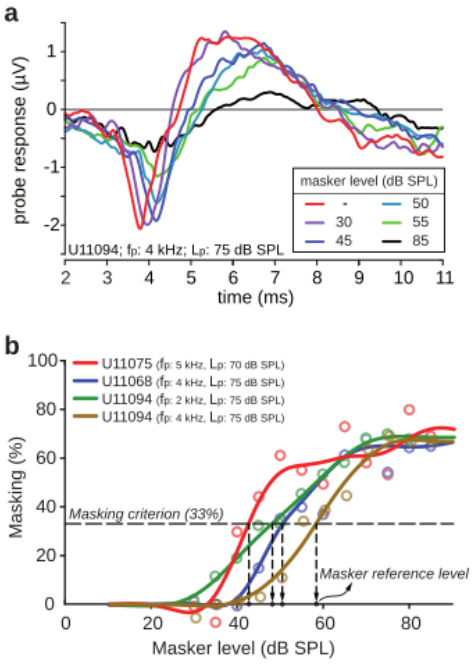

Verschooten et al. 2018 (humans)

Figure 10: Forward masking: masking of CAP as a function of probe level (in case of Verschooten et al.: broadband noise). Sometimes fit by a Weibull function

2 Idea

General idea: return to the 'double convolution' model but exploit different forward masking settings to have a more robust model of CAP (and possibly estimate auditory tuning)

$$CAP = \underbrace{E \star NPST}_{CPST} \star UR$$

(notations of [Bappert et al., 1980]). Or:

$$CAP = E \star H$$

where E is the 'excitation pattern' and $H = NPST \star UR$. It's a 'blind deconvolution' problem because we have only a vague idea of what E and H are.

With forward masking, we can get more information. Instead of having a single excitation pattern E, we can have several patterns

$$E_i = M_i(\theta) \cdot E_0$$

where $M_i(\theta)$ is a masking pattern depending on the masker (tone, band noise..), and E_0 is the raw excitation pattern (without masking). The masking pattern depends on the model parameters θ which are primarily the latencies and the frequency selectivity (given a simple model of auditory filters). We can compute a theoretical 'masking pattern' thanks to the plot of % masking as a function of masker level for broadband noise, see Fig. 10 (under certain assumptions, e.g. have to be careful of growth-of-masking).

Then now we have a system of equations with

$$[CAP]_i = [M_i(\theta) \cdot E_0]_i \star H \ .$$

It is still the 'blind deconvolution' problem but we have a stronger prior on the excitation patterns as they belong to a linear subspace parametrized by E_0. Simple projection-based algorithms exist in this case [Yang et al., 1994] (this is essentially deconvolution done alternatively on E and H with a projection step between two iterations). Note: prior constraints could be also put on H based on what we know about UR and NPST, but this seems more challenging (maybe as a second step). We can also think of a regularity prior on E_0.
idea: initialize the algorithm with reasonable estimations of E and H. At the end of the algorithm, done for each set of parameters θ, we would select the best model minimizing the square error, then see how it behaves compared to real data.

Toy model: Masked CAP toy model.ipynb
Possibility of first step? try to see if estimation works on simple simulated data like this one

- TODO, next week : more on type of makser/probes, hypotheses, questions and difficulties

References

Paul J Abbas and Michael P Gorga. AP responses in forward-masking paradigms and relationship to responses of auditory-nerve fibers. *The Journal of the Acoustical Society of America*, 69(2):492–499, 1981. ISSN NA. doi: 10.1121/1.385477. URL https://doi.org/10.1121/1.385477http://scitation.aip.org/content/asa/journal/jasa/69/2/10.1121/1.385477.

E. Bappert, M. Hoke, and B. Lütkenhöner. Deconvolution of compound action potentials and nonlinear features of the PST histogram. *Hearing Research*, 2(3-4):573–579, jun 1980. ISSN 03785955. doi: 10.1016/0378-5955(80)90095-7.

J. J. Eggermont. Analysis of compound action potential responses to tone bursts in the human and guinea pig cochlea. *Journal of the Acoustical Society of America*, 60(5):1132–1139, nov 1976. ISSN NA. doi: 10.1121/1.381214. URL http://www.ncbi.nlm.nih.gov/pubmed/977839.

Jos J. Eggermont. Ups and downs in 75 years of electrocochleography, jan 2017. ISSN 16625137.

R V Harrison, J.-M Aran, and M Negrevergne. The Frequency Selectivity of the Normal and Pathological Human Cochlea. Technical report, 1981a.

Robert V. Harrison, Jean–Marie Aran, and Jean–Paul Erre. AP tuning curves from normal and pathological human and guinea pig cochleas. *The Journal of the Acoustical Society of America*, 69(5):1374–1385, may 1981b. ISSN 0001-4966. doi: 10.1121/1.385819. URL http://asa.scitation.org/doi/10.1121/1.385819.

N. Y. S. Kiang, E. C. Moxon, and A. R. Kahn. The Relationship of Gross Potential Record from the Cochlea to Single Unit Activity in the Auditory Nerve. In *Electrocochleography*, pages 95–115. 1976.

Özcan Özdamar and Peter Dallos. Synchronous responses of the primary auditory fibers to the onset of tone burst and their relation to compound action potentials. *Brain Research*, 155(1):169–175, oct 1978. ISSN 00068993. doi: 10.1016/0006-8993(78)90320-7.

Vera F. Prijs. Single-unit response at the round window of the guinea pig. *Hearing Research*, 21(2):127–133, jan 1986. ISSN 03785955. doi: 10.1016/0378-5955(86)90034-1.

Evan M. Relkin and Robert L. Smith. Forward masking of the compound action potential: Thresholds for the detection of the N1 peak. *Hearing Research*, 53(1):131–140, 1991. ISSN 03785955. doi: 10.1016/0378-5955(91)90220-4.

Eric Verschooten, Luis Robles, Damir Kovačić, and Philip X Joris. Auditory nerve frequency tuning measured with forward-masked compound action potentials. *JARO - Journal of the Association for Research in Otolaryngology*, 13(6):799–817, 2012. ISSN 15253961. doi: 10.1007/s10162-012-0346-z. URL https://www.ncbi.nlm.nih.gov/pmc/articles/PMC3505591/pdf/10162{_}2012{_}Article{_}346.pdf.

Eric Verschooten, Christian Desloovere, and Philip X. Joris. High-resolution frequency tuning but not temporal coding in the human cochlea. *PLOS Biology*, 16(10):e2005164, oct 2018. ISSN 1545-7885. doi: 10.1371/journal.pbio.2005164. URL http://dx.plos.org/10.1371/journal.pbio.2005164.

Binseng Wang. *The relation between the compound action potential and unit discharges of the auditory nerve.* PhD thesis, MIT, 1979.

Yongyi Yang, NP Galatsanos, and Henry Stark. Projection-based blind deconvolution. *Journal of the Optical Society of America A*, 11(9):2401–2409, 1994.